Biosensors and Bioelectronics 214 (2022) 114520

Contents lists available at ScienceDirect

Biosensors and Bioelectronics

journal homepage: www.elsevier.com/locate/bios

# Coupling split-*lux* cassette with a toggle switch in bacteria for ultrasensitive blood markers detection in feces and urine

Zhen-Ping Zou [a], Ying Yang [a], Junshan Wang [b], Ying Zhou [a,**], Bang-Ce Ye [a,c,*]

[a] Laboratory of Biosystems and Microanalysis, State Key Laboratory of Bioreactor Engineering, East China University of Science and Technology, Shanghai, 200237, China

[b] Department of Gastroenterology, The Shanghai Tenth Peoples Hospital, Tongji University, Shanghai, 200072, China

[c] Institute of Engineering Biology and Health, Collaborative Innovation Center of Yangtze River Delta Region Green Pharmaceuticals, College of Pharmaceutical Sciences, Zhejiang University of Technology, Hangzhou, Zhejiang, 310014, China

ARTICLE INFO

*Keywords:*
Gene circuit
Whole-cell biosensors
Heme detection
Split-*lux* cassette
Toggle switches

ABSTRACT

Cell-based biosensors have powerful abilities to sense a variety of signal chemical molecules. However, compared with commercialized methods, whole-cell biosensors cannot meet the requirements for the lower sensitivity and faster response. Here, we reprogrammed a gene circuit by coupling split-*lux* cassette with a toggle switch for detecting heme ultra-sensitively. The resultant biosensor (named YES601) exhibited improved detection limit (0.12 ppm) and satisfied maximum induction ratio (more than 4000 folds) for lysed blood detection. Furthermore, we harnessed YES601 to detect the blood signal in the human urine and feces from the mice with DSS-induced colitis, and the results indicated that YES601 showed more satisfied sensitivity and maximum induction ratio compared with chemical method. This ultrasensitive blood biosensor will be applied to detect trace blood *in vitro* for early-stage diagnosis of serious diseases, and aiding the rapid development for application in diagnosis *in vivo* in the future.

## 1. Introduction

As an alternative strategy to electronic or chemical sensors, whole-cell biosensors (WCBs) provide a cost-effective and environmentally friendly way to detect and report biomarkers or conditions of interest. Although the construction of WCBs is laborious, its subsequent use and mass production are very simple and convenient. The other attractive feature of WCBs is the flexibility design and outputs, because WCBs can be tailored to the specific application (such as genetic logic gates). Furthermore, compared to sensors based on inanimate components, WCBs are easier to deploy in complex environments. (Hicks et al., 2020; Valle et al., 2020). Owing to their innate robust functionality in complex environments, more and more WCBs have been harnessed to various applications ranging from environmental monitoring (Moraskie et al., 2021; Sahu et al., 2022), molecular record (Tang and Liu, 2018; Zou and Ye, 2020) and bioproduction (Hossain et al., 2020; Mitchler et al., 2021) to disease diagnosis and treatment for human health (Riglar and Silver, 2018; Landry and Tabor, 2017; Zhou et al., 2020). However, most of WCBs still have some limitations compared with the existing methods, such as sensitivity, leakage, operating range and so on. It is worth noting that the sensitivity is one of the most important characteristics of the sensor in practical application for the concentration of target is usually extremely low.

To address these bottlenecks, synthetic biology has been utilized to develop abundant genetic circuits and elements to improve the performance of the WCBs (Nielsen et al., 2016; Ding et al., 2021; Wan et al., 2019a; Roquet and Lu, 2014). Some researchers tried to optimize the genetic modules, including the intracellular concentration of transcription factors at the transcriptional (Chen et al., 2018), translational (Clifton et al., 2018; Jiang et al., 2020) and post-translational levels (Cameron and Collins, 2014), directed evolution of transcription factors (Javanpour and Liu, 2021), selection of reporters and optimization of their expression levels (Lopreside et al., 2019; Hynninen et al., 2020) and selection of plasmid backbones and hosts (Tas et al., 2021). Furthermore, they optimized the design of genetic circuits, such as toggle switches (Gardner et al., 2000), logic gates (Schladt et al., 2021),

* Corresponding author. Laboratory of Biosystems and Microanalysis, State Key Laboratory of Bioreactor Engineering, East China University of Science and Technology, Shanghai, 200237, China.

** Corresponding author.

*E-mail address:* bcye@ecust.edu.cn (B.-C. Ye).

https://doi.org/10.1016/j.bios.2022.114520

Received 19 April 2022; Received in revised form 24 June 2022; Accepted 26 June 2022

Available online 30 June 2022

genetic amplifiers (Wan et al., 2019b), and DNA sponges (Wan et al., 2020), which can effectively adjust the response curves of the biosensors. However, most studies were aimed at improving a certain performance, such as limit of detection (LOD) by reducing the intracellular concentration of the repressor protein, which leading to a high background signal and the reduction of the dynamic range. Consequently, the rational comprehensive design should be moved forward to make a trade-off between different sensing features for further practical applications.

In this study, we designed and optimized an ultrasensitive biosensor to detect heme. As a critical biological molecule, heme is an important component of red blood cells (RBCs). The detection of heme levels can indicate the possible presence of free hemoglobin or blood (hemoglobinuria or hematuria) in urine and occult blood in feces. As known, fecal occult blood is caused by gastrointestinal diseases (Flynn and Eisenstein, 2019; Mandel et al., 2000), and hematuria is caused by serious diseases such as kidney disease, bladder cancer, and urinary tract infection (Feld et al., 1997). Therefore, trace blood test in urine and fecal occult blood detection are important indicators in clinical physical examination, which are the crucial targets for early-stage diagnosis and treatment. Nowadays, chemical methods are utilized for the detection of bloody stool, which can detect $2 \times 10^4$ to $1 \times 10^6$ RBCs per mL of urine (Freni et al., 1977). However, such tests often yield false-positive results when the samples are contaminated with vitamin C, peroxidase or myoglobin from damaged muscle cells (Veerreddy, 2013). Furthermore, in order to detect the trace blood in urine, microscopy and dipstick tests are carried out to count the number of red blood cells, which may cause false negative results. Using electrical signals to detect blood in urine has also been reported, but this method requires complex preprocessing and sophisticated equipment (Nasir et al., 2019). Recently, Natalia et al. developed a heme-responsive WCB capable of detecting $5 \times 10^5$ RBCs per mL of simulated urine (Barger et al., 2021), but the LOD was about ten times higher than the chemical one. Therefore, it is necessary to further improve the sensitivity of the heme-responsive WCB and demonstrate the performance of the sensor in actual fecal and urine samples to judge whether it meets the requirements of practical applications.

To this end, we controlled the transcriptional and translational levels of heme-responsive protein (HrtR) to reduce leaky expression, and improved LOD and maximum signal output through engineered promoter modifications of reporter gene. Furthermore, coupling split-*lux* cassette with a toggle switch was carried out to promote sensitivity and maximum induction ratio (MIR) significantly. It was worth noting that the most sensitive heme-responsive WCB (YES601) was obtained with LOD of 0.12 ppm and the MIR of more than 4000 folds. YES601 could detect fecal occult blood on the second day, while chemical one was only present in the third day sample. In human urine samples, the lowest detection limit of YES601 was 0.25 ppm while the o-tolidine method was more than 7.5 ppm. As far as we know, YES601 exhibited the lowest heme detection limit of reported data so far. We demonstrated that this work provided a global design strategy to achieve the optimal biosensor parameters, which offers a greater possibility for further practical applications in health care.

## 2. Material and methods

### 2.1. Strains, plasmids, culture conditions and chemical

All plasmids were performed in *E. coil* DH5α. Strains were cultured in lysogeny broth (LB) medium, with appropriate antibiotics: streptomycin (50 μg/mL), chloramphenicol (25 μg/mL), and ampicillin (100 μg/mL). The engineered EcN were grown at 37 °C overnight in a microplate shaker at 1000 rpm in 800 μL of LB, supplemented with appropriate antibiotics to activate strains. For liquid induction, the cells were diluted 200-fold or 1000-fold in 200 μL LB medium containing different concentrations of inducer and then incubated in a microplate shaker with continuous shaking (1000 rpm, 37 °C). After 8 h, unless otherwise indicated, the fluorescence, luminescence and absorbance at optical density 600 nm ($OD_{600}$) were detected. For luminescence dynamic analysis: (1) The cells were diluted 200-fold or 1000-fold in 200 μL LB medium (Using plates with white edge on clear bottom) containing different concentrations of inducer and then shake the cultures in the microplate reader (37 °C), and bioluminescence signals were read at 1 min intervals for 60/120 min or 1 h intervals for 5 h (2) The cells were diluted 200-fold in 100 μL LB medium and cultured for 2 h ($OD_{600} \approx 0.3$), then supplemented with 100 μL of fresh LB medium containing different concentrations of inducers to continue the culture and bioluminescence signals were read at 1 min intervals for 45/60 min or 30 min intervals for 120 min.

A stock solution of ferric chloride heme (Sigma-Aldrich) was prepared by dissolving hemin powder in 1 M NaOH to a concentration of 25 mM, diluting with $ddH_2O$ to a final concentration of 1 mM. All reagents were filtered using 0.22 μm syringe filters. Human blood and urine were supplied by Shanghai Tenth People's Hospital. Whole blood was lysed by red blood cell (RBC) lysis buffer for 10 min.

### 2.2. Gene circuit construction and genome cloning

The sequences of all parts are shown in Table S1. Basic molecular cloning techniques were used to construct plasmids containing heme-responsive genetic circuits and toggle switches. A prototype heme-sensing plasmid (pMM643) was purchased from Addgene, USA. The reporter *luxCDABE*, kanamycin resistance gene, and replication origin were replaced by *sfGFP*, streptomycin resistance gene, and pSC101 origin of replication, respectively, to get the pWT-Hem. The *fhtR*, *pefR* and *hatR* were synthesized by Tsingke Biotechnology (China, Bei Jing). All gene fragments were got via polymerase chain reaction (PCR) amplification and recombinant plasmids obtained by homologous recombination, the recombinant products were transformed into *E. coli* DH5α by heat shock. The correct cloning was selected by LB agar plates with 50 mg/mL streptomycin and then verify by sequencing.

The λ-Red recombination method was used to knock out the endogenous genes (*lacI and lacZ*) from EcN by the units of *lux* cassette. The operation process follows the protocol of Zou et al. (Zou and Ye, 2020). And the clones with correct genome insertion was selected by LB agar plates with 25 mg/mL chloramphenicol.

### 2.3. Determination of fluorescence/luminescence intensity

For detecting the fluorescence signals, the culture samples were washed with PBS and then resuspended in double volume of PBS. 200 μL washed sample was added to a 96-well clear plate and 100 μL washed samples was added to a black 384-well black plate. $OD_{600}$ and fluorescence (excitation at 480 nm, emission at 500–600 nm) was read by microplate reader (BioTek Instruments, Winooski, VT, USA). Fluo/$OD_{600}$ shows the normalized sfGFP expression. The culture aliquots were read by microplate reader at 490 nm for detecting the luminescence signals and read the $OD_{600}$ as well, RLU/$OD_{600}$ shows the normalized luminescence signals.

### 2.4. DSS-induced mouse colitis model and fecal occult blood test

Male C57BL/6 mice (Southern model, China) aged 6–8 weeks were used in this study. The mice were housed at a standard temperature (20–22 °C) and 12-h light/12-h cycle for one week. And then randomly divided into two groups, DSS (MW=36,000–50,000; MP Biomedicals) was added at a final concentration of 3% to their drinking water for 5 days to induce colitis (drinking water ad libitum). The control mice were drunk untreated water freely.

Mouse fecal samples were collected every day for seven days since the day before DSS treatment, and the collected fecal samples were homogenized by PBS (1g sample was homogenized with 10 mL PBS).

The homogenized samples were centrifuged at 4°C for 10 min and then the supernatant was collected and filtered by 0.22 μm syringe filters to obtain the samples to be tested (stool aliquots).

The chemical method: 50 μL of o-tolidine and 50 μL of $H_2O_2$ were added to 1 μL of the stool aliquots and then observed the color change and read $OD_{600}$ after 5min incubation. The WCBs method: 1 μL of the stool aliquots were added to the 200 μL medium containing 1/1000 YES601 and cultured for 4 h to detect bioluminescence and $OD_{600}$. RLU/$OD_{600}$ shows the normalized luminescence signals.

### 2.5. Detection of blood markers in human urine

The composition of the tested samples are as follows: 2.5% LB powder was dissolved in human urine with different lysed blood concentrations. The chemical method: 50 μL of o-tolidine and 50 μL of $H_2O_2$ were added to 50 μL of the test samples and $OD_{600}$ was read after 5 min. The WCBs method: YES601 was incubated in the test samples at 1/1000 dilution for 4 h (37 °C, 1000 rpm), and then measured the $OD_{600}$ and bioluminescence. RLU/$OD_{600}$ shows the normalized luminescence

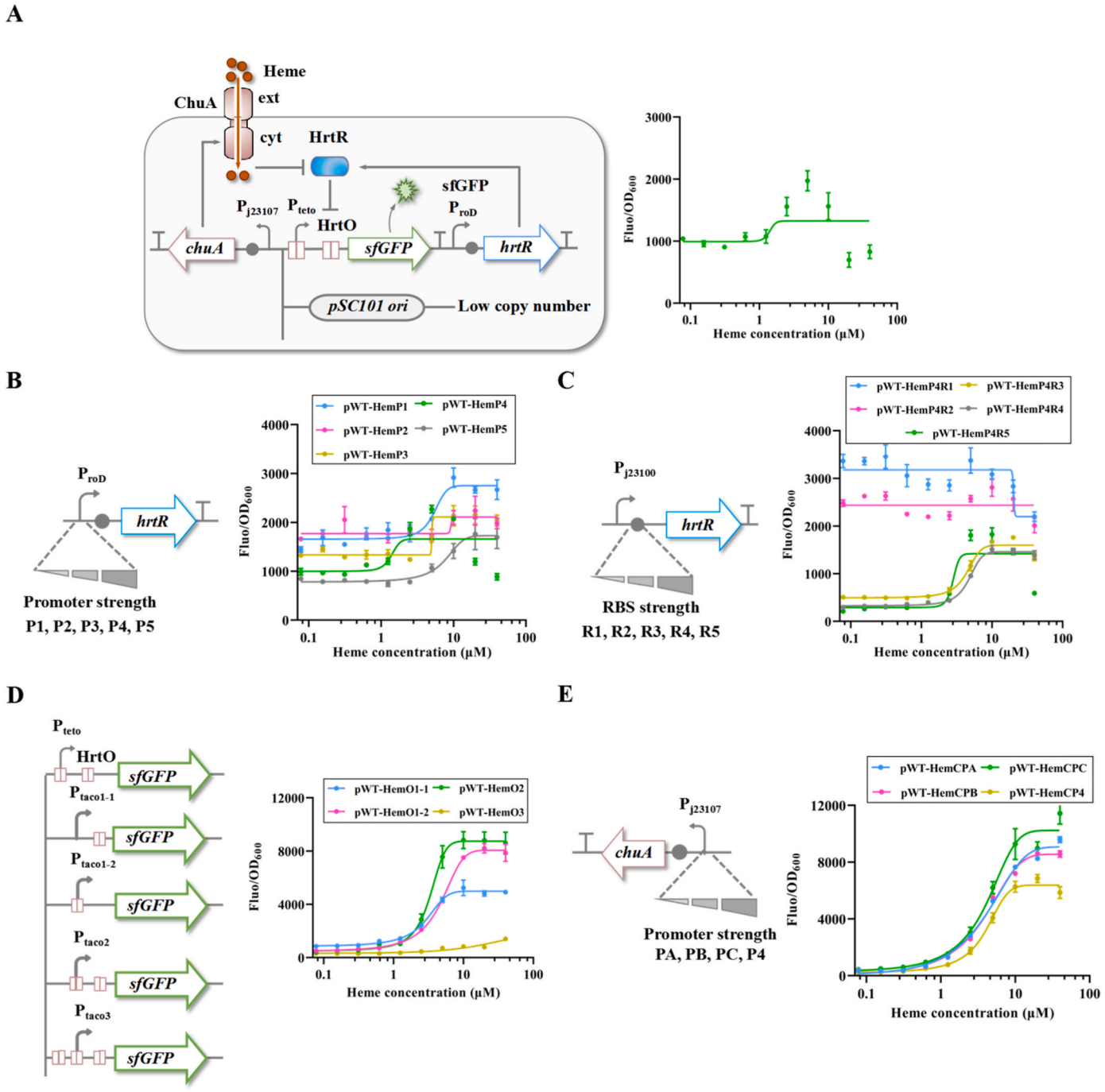


**Fig. 1.** Design and characterization of heme-responsive whole-cell biosensors. (A) Constructing and characterization of the prototype heme-responsive genetic circuit in EcN. B) Characterization of a set of constitutive promoters having different transcriptional strengths to express *hrtR* gene in response to various heme concentrations. (C) Characterization of a set of RBSs having different translational strengths to express HrtR protein in response to different concentrations of heme. (D) Enhancing the transcription level of reporter genes and altering the number of HrtR operators to modulate sensor performance. (E) Tuning outer-membrane transporter ChuA's transcript level by varying the strength of promoter to improve the transport efficiency of heme. The data are presented as the mean ± SEM (n=3).

signals.

## 3. Results and discussion

### 3.1. Optimization and examination of heme-responsive genetic circuits using fluorescent protein

Most heme biosensors were operated on high/medium-copy-number plasmids, which increased metabolic burden and lead to genetic instability (Barger et al., 2021; Mimee et al., 2018). In order to address this issue, we placed the heme-responsive gene circle on a low-copy-number plasmid with pSC101 origin of replication (5–10 copies per bacterium), named pWT-Hem. The heme-responsive transcriptional repressor HrtR (Lechardeur et al., 2012) from *Lactococcus lactis* and a transporter ChuA (Nobles et al., 2015) from *Escherichia coli* O157:H7 were expressed under constitutive promoters $P_{roD}$ and $P_{j23107}$, respectively. The output signal was superfolder green fluorescent protein (sfGFP) regulated by a promoter containing two repressor sites (Fig. 1A, left). We used the probiotic *E. coli* Nissle 1917 (EcN) as the chassis cell (Westendorf et al., 2005), and the biosensor's ability was tested to respond to various heme concentrations. The strain with pWT-Hem could only sense over 2.5 μM heme, and fluorescence intensity only was induced 1.9-fold by 5 μM heme, as a result of high leaky expression in the absence of heme (Fig. 1A, right).

In order to improve sensor performance, we tuned intracellular level of repressor protein HrtR by different promoters. The $P_{roD}$ of the prototype plasmid pWT-hem was replaced upstream of *hrtR* by five constitutive promoters (P1: $P_{j23115}$; P2: $P_{j23105}$; P3: $P_{j23106}$; P4: $P_{j23100}$; P5: $P_{j23119}$) of normalized strengths (http://parts.igem.org), to adjust the transcription level respectively (Fig. 1B). The results showed that the weaker the promoter was, the higher leaky expression would be. As shown in Fig. 1B, pWT-HemP4 was chosen for the subsequent optimizing experiments for the lowest LOD, although the background expression was higher than pWT-HemP5.

We next employed various RBS sequences (R1: BBa_B0031; R2: BBa_B0032; R3: BBa_B0029; R4: BBa_B0034; R5: BBa_B0035) with different intensities (http://parts.igem.org) to control the translational level of HrtR protein (Fig. 1C). The results indicated that the stronger the RBS was, the lower leaky expression could be. The pWT-HemP4R5 showed the lowest leaky expression (213.2 Fluo/$OD_{600}$) and the highest MIR (8.6-fold) while the LOD was 1.25 μM.

To further improve the LOD and MIR for practical utilization, we replaced the *tet* promoter by a stronger one ($P_{tac}$) to increase the sfGFP expression level (Fig. 1D, left). Meanwhile, altering the number and the locations of the operator sites increased the efficiency of the repressor, which led to reducing the background leakage greatly (Fig. 1D). As expected, the *tac* promoter significantly enhanced the output dynamic range, and the addition of the second operator site reduced leakage obviously. The sensor with two operators (a HrtR operator within $P_{tac}$ and an additional one further downstream from $P_{tac}$), named pWT-HemO2, showed the best performance compared with others. Fig. 1D showed that the background expression of EcN, harboring pWT-HemO2, was 425.7 Fluo/$OD_{600}$, the maximum output expression reached at 8803.0 Fluo/$OD_{600}$, the MIR was 20.7-fold, and the LOD decreased to 0.31 μM. Not only that, the optimized sensor also relieved the toxicity of heme to the bacteria (Fig. S1).

As known, another vital factor affecting the biosensor sensitivity is increasing the targets concentration (Cayron et al., 2017). To increase the intracellular level of heme, we replaced the promoter J23107 controlling the transcription of *chuA* by four constitutive promoters with different expression intensities (PA: $P_{j23108}$; PB: $P_{j23111}$; PC: $P_{j23104}$; P4: $P_{j23100}$) (Fig. 1E, left). A dose-response curve of the four biosensors was obtained after incubating them with heme for 8 h. Fig. 1E showed that when the amount of ChuA exceeded a certain range, it could not improve the signal intensity, but decreased the signal conversely. The pWT-HemCPC showed the lowest background expression (431.0 Fluo/$OD_{600}$), the highest output (11433.9 Fluo/$OD_{600}$), the MIR was 26.5-fold and the LOD was 0.31 μM. We incubated $1 \times 10^9$ CFU of three strains (pWT-HemO2, pWT-HemCPA, pWT-HemCPC) with 5 μM heme for 2 h, respectively, and then detected the intracellular heme level of each culture. The results showed that increasing the transcription level of *chuA* could improve the uptake of heme by the engineered bacteria (Fig. S2). We also tested heme-responsive proteins from *Enterococcus faecalis* (Saillant et al., 2021), *Streptococcus agalactiae* (Nishinaga et al., 2021), and *Clostridium difficile* (Knippel et al., 2018). And only the HrtR exhibited the best sensing performance (Figs. S3A and B).

In this section, we regulated the intracellular concentration of HrtR and ChuA by the transcriptional and translational levels, respectively. In addition, we increased the transcription level of the reporter gene *sfGFP* and the efficiency of the repressor by altering the number and locations of the operator sites. After step-by-step optimization, we obtained a sensor plasmid pWT-HemCPC which LOD was 0.31 μM, and MIR was 26.5-fold.

### 3.2. Design and characterization of heme-responsive gene circles by completely split of lux cassette to detect the lysed blood

sfGFP is commonly used as a reporter, but its light emission must be read by a fluorimeter machine. However, bioluminescent reporters are much more sensitive, fast-response and convenient without using external substrates compared with sfGFP (Close et al., 2012). The bacterial luciferase gene cassette contains *luxC*, *luxD*, *luxA*, *luxB*, *luxE*. The luciferase protein is a heterodimer formed by LuxA and LuxB. The *luxC*, *luxD*, and *luxE* gene encode for a reductase, transferase, and synthase, respectively, which work together for the bioluminescent reaction (Meighen, 1991). However, transcription and translation of a large *lux* operon is inefficient, and it is difficult to manipulate the long operon on one plasmid. Some studies used the luciferase *lux AB* as a reporter (Meighen, 1991). However, this design requires the addition of a metabolic substrate for luciferase. Some studies tried to split the *luxCDABE* into two parts, (*luxAB* and *luxCDE*) to improve bioluminescent reporter performance (Yagur-Kroll and Belkin, 2011; Barger et al., 2019).

To further improve the performance of heme-responsive WCBs and simplified the sensor plasmids, we completely split and reassembled the *lux* cassette in EcN, which generated five combinations of sensing systems (Fig. S4 and Fig. 2A). The units of *lux* in plasmid were induced by heme and the *lacI* and *lacZ* genes of EcN were replaced by the *lux* unit (constitutively expressed by tac promoter) which was knocked-in the genome. The strains were pre-cultured for 2 h, then added the fresh medium containing different concentrations of heme, and the luminescence signals were measured at 90 min (Fig. 2B, left). Induction fold was the ratio of normalized luminescence signal in the presence of 20 μM heme to background signal (Fig. 2B, right). The results showed that EcNABDE-luxC had the lowest LOD (0.16 μM), the lowest leaky expression (202.8 RLU/$OD_{600}$), and the highest MIR (273.9-fold) compared with the other four combinations. Further, we examined the time-response of EcNABDE-luxC in LB medium containing heme with various concentrations. Fig. 2C showed that a significant bioluminescence signal could be observed in 20 min (Fig. 2C). In order to investigate the blood detecting ability of EcNABDE-luxC, we lysed blood by RBC lysis buffer for 10 min to obtain samples to be tested. The pre-cultured (2 h) EcNABDE-luxC cells were mixed with deferent concentrations of lysed blood which dissolved in LB medium, and kept shaking for 120 min (Fig. 2D). Bioluminescence and $OD_{600}$ were read at 30 min intervals for 120 min. Luminescence values increased after the exposure to different concentrations of lysed blood and reached the maxima after 60 min. Luminescence intensity increases with increasing inducer concentration (Fig. 2E). Using the ECL imaging system, it was obviously observed that the luminescence signal enhanced along with the increasing of lysed blood concentration (Fig. 2F).

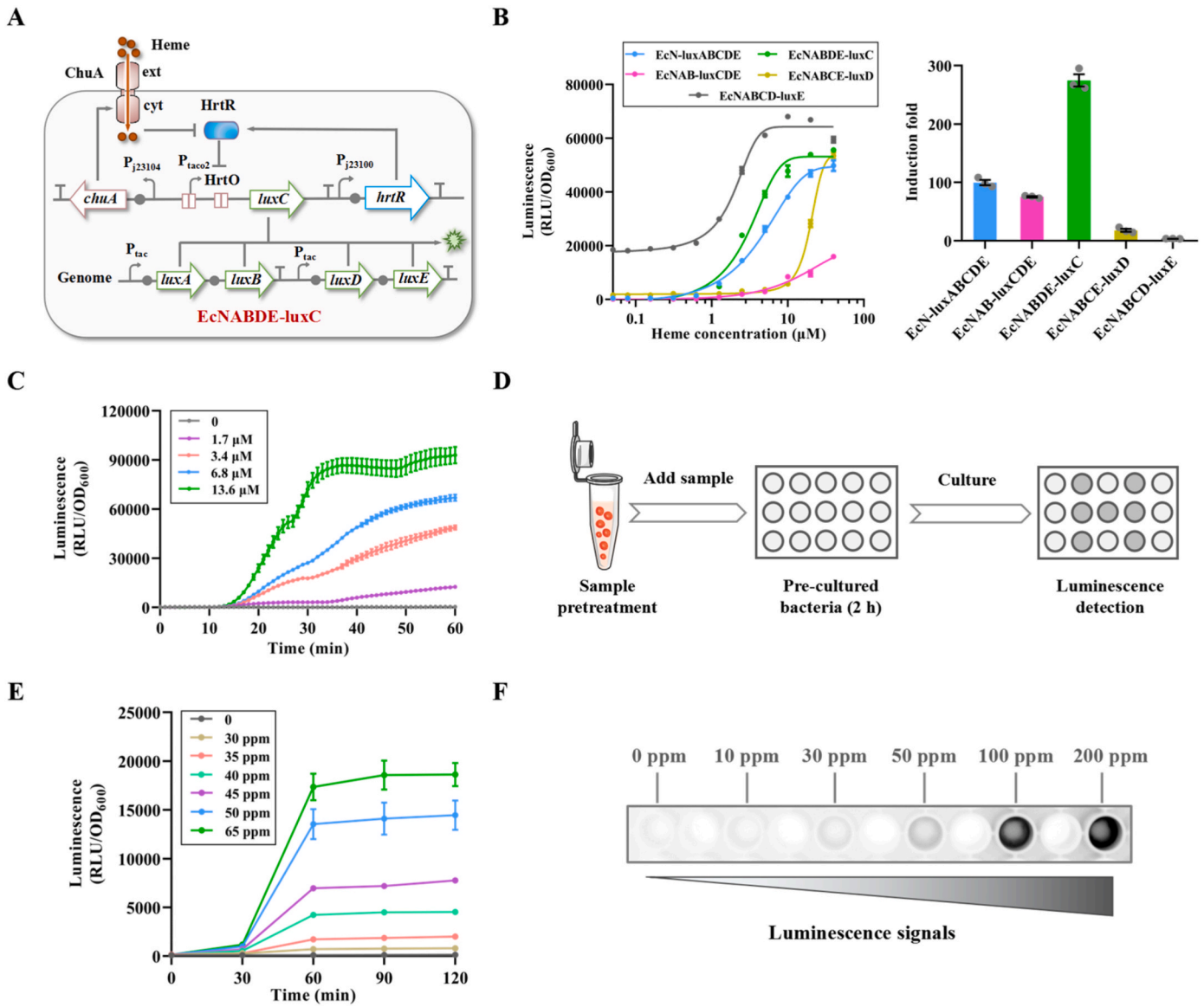


**Fig. 2.** Design and development of heme-responsive WCBs by completing split of *lux* cassette to detect the lysed blood. (A) Circuit diagram of the heme-sensor in EcNABDE-luxC strain. (B) Characterization of the dose-response curves (left) and induction fold (right) of different heme-responsive sensors. (C) The time-responses of EcNABDE-luxC after exposure to heme, which presented as normalized bioluminescent signals (RLU/$OD_{600}$). Pre-cultured bacteria were induced by different concentrations of heme. Luminescence signals were read at 1 min intervals for 60 min and $OD_{600}$ was read at 60 min. (D) The detect process of red blood cells by WCBs. (E) The time-responses of EcNABDE-luxC after exposure to lysed blood in LB medium, which presented as normalized bioluminescent signals (RLU/$OD_{600}$). Pre-cultured bacteria were induced by different concentrations of lysed blood (0–65 ppm), and bioluminescence signals and $OD_{600}$ were read at 30 min intervals for 120 min. (F) Visualization of bioluminescent signals. Pre-cultured bacteria were induced by different concentrations of lysed blood (0–200 ppm) for 60 min, and then observed the luminescence by ECL imaging system. The data are presented as the mean ± SEM (n=3).

### *3.3. Coupling split-lux cassette with a toggle switch to lower detection limits for heme/blood*

To demonstrate the application of EcNABDE-luxC in physiological samples, we should move on improving its sensitivity. As the beginning of modern synthetic biology, the toggle switch was composed of two repressors (repressor 1 and repressor 2) which were triggered by two constitutive promoters (promoter 1 and promoter 2), respectively. Each promoter was repressed by the repressor that was transcribed by the opposing promoter (Fig. S5). Collins et al. (Gardner et al., 2000). Established the following dimensionless model to understand the behavior of the toggle switch and the conditions for bistability.

$$\frac{du}{dt} = \frac{\alpha_1}{1+v^{\beta}} - u$$

$$\frac{dv}{dt} = \frac{\alpha_2}{1+u^{\gamma}} - v$$

Where $u$ and $v$ are the concentrations of repressor 1 and repressor 2, respectively, $\alpha_1$ and $\alpha_2$ are the effective rates of repressor 1 and repressor 2, respectively, and $\beta$ and $\gamma$ are the cooperativity of repression of promoter 1 and promoter 2 (Gardner et al., 2000). Once the circle is triggered by a specific stimulus, the rapid transition between the two states provides easily distinguishable "on" and "off" phases.

We designed a toggle switch based on the repressor HrtR and LacI in DH5α strain, and used the sfGFP as a reporter (Fig. S6A). To investigate the conditions required for stability, six variants of the toggle switch

were constructed by inserting six RBS sequences of different strengths into the upstream of the *lacI* gene. The strains were grown in LB for 12 h, and then the cultures were washed and diluted into fresh LB medium with IPTG of different concentrations for 12 h cultivation. After that, the cultures were washed and diluted into fresh LB medium for 2 passages (12 h/passage). We measured the fluorescence intensity of the cultures at each time point. The results showed that the stronger the RBS is, the higher background is (Figs. S6B–G). Although leaky expression could be reduced by adding IPTG, the steady state could not be achieved simultaneously. We speculated that the endogenous unregulated LacI protein in the DH5α genome affected the toggle switch to get steady state.

Therefore, we transplanted the toggle switch with "None" or "B0033" RBS, into EcNABDE strain, in which the *lacI* and *lacZ* genes were replaced by the *luxABDE* gene (Fig. S7A). Through the previous experimental procedure, we examined the stability of two sensors. (Fig. S7B). The results showed that the toggle switch containing "None" RBS could maintain stability with a lowest leaky expression, while "B0033" only maintained stable state within two passages. And then we coupled split-*lux* cassette with the optimized toggle switch in bacteria, which generated a strain named YES601 (Fig. 3A). The YES601 (with a toggle switch) and EcNABDE-luxC (without a toggle switch) were compared under the induction of various heme concentrations (Fig. 3B), and the YES601 strain could response 0.019 μM heme ($LogEC_{50}$ = 0.0718), which was 10-fold improved than the control one ($LogEC_{50}$ = 0.8692). The dose-response curve of YES601 for lysed blood showed that blood could be detected as low as 0.12 ppm ($LogEC_{50}$ = 1.770) in LB medium when bacterial cells were diluted at 1/1000, the leaky expression lower to 4.3 RLU/$OD_{600}$, and the MIR is 4047.4-fold (Fig. 3C). We then performed a time-response analysis of the engineered bacteria, and the luminescence signal reached maximum at 4 h (Fig. 3D). More accurate time-response curves showed that the luminescence signal started to increase at 50 min, and the sample detection could be completed within 120 min (Fig. 3E). The above two time-response curves were detected under the condition that bacterial cells were inoculated at 1/1000. To investigate the shortest responsive time of YES601 to blood, we pre-cultured the engineered bacteria for 2 h and then replaced the medium by fresh LB medium containing 30 ppm blood. Bioluminescence values could be detected in 20 min after the exposure to blood and the sample detection could be completed within 50 min (Fig. 3F). In conclusion, by combining the split-*lux* cassette with a well-designed toggle switch, we obtained an engineered strain named YES601 that could respond to lysed blood as low as 0.12 ppm, and detect 1 ppm lysed blood in 100 min and 30 ppm in 30 min, respectively.

### 3.4. Early detection of fecal occult blood in DSS-induced colitis mice model by YES601

The detection of fecal occult blood plays a crucial role in the early diagnosis and treatment of gastrointestinal diseases. We constructed DSS-induced colitis mice model mice to demonstrate that engineered bacteria YES601 could detect fecal occult blood earlier than chemical method. From the day before DSS treatment, mouse fecal samples were collected every day for seven days (Fig. 4A), and the collected fecal samples were homogenized and the supernatant was collected and

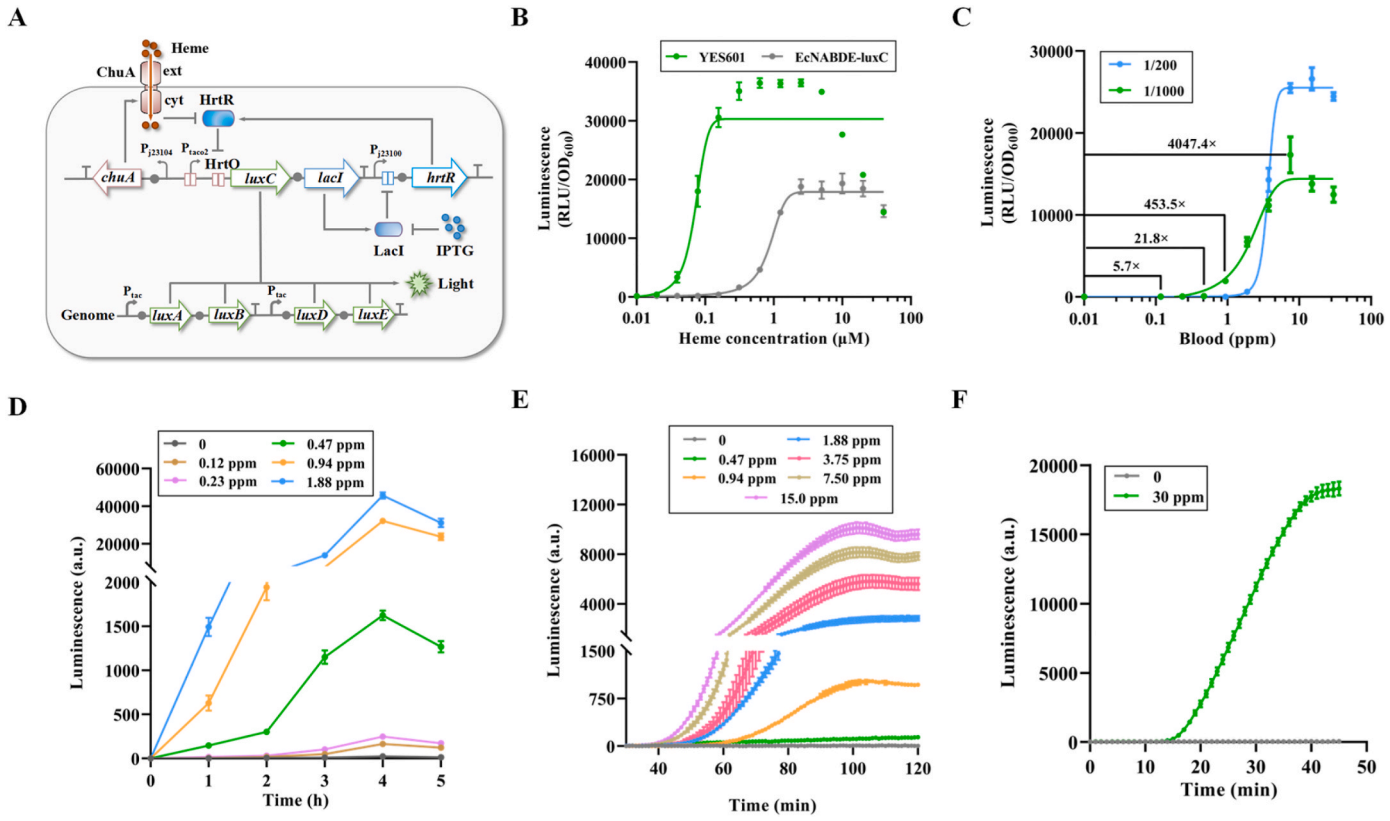


**Fig. 3.** Coupling split-*lux* system with a toggle switch for ultrasensitive detection of heme/blood. (A) Schematic diagram of the toggle switch using the split *lux* system as the reporter gene in EcNABCD which the *lacI* and *lacZ* genes were replaced by *luxABDE*. (B) Characterization of the dose-response curves of YES601 and EcNABDE-luxC induced by various heme concentrations. (C) The dose-responses of YES601 after exposure to lysed blood under the condition of different inoculum dose. Bacterial cells were incubated with different concentrations of inducers for 4 h and then detect the luminescence to get the dose-responses. (D) The time-responses of YES601 after exposure to various lysed blood concentrations (0–1.88 ppm) in LB medium. (E) The more accurate time-responses of YES601 after exposure to various lysed blood concentrations (0–15 ppm) in LB medium, and bioluminescence signals were read at 1 min intervals for 120 min. (F) Investigating the shortest response time of YES601 to blood. Pre-cultured bacteria was induced by 30 ppm of lysed blood, and bioluminescence signals was read at 1 min intervals for 45 min. The data are presented as the mean ± SEM (n=3). a.u., arbitrary units.

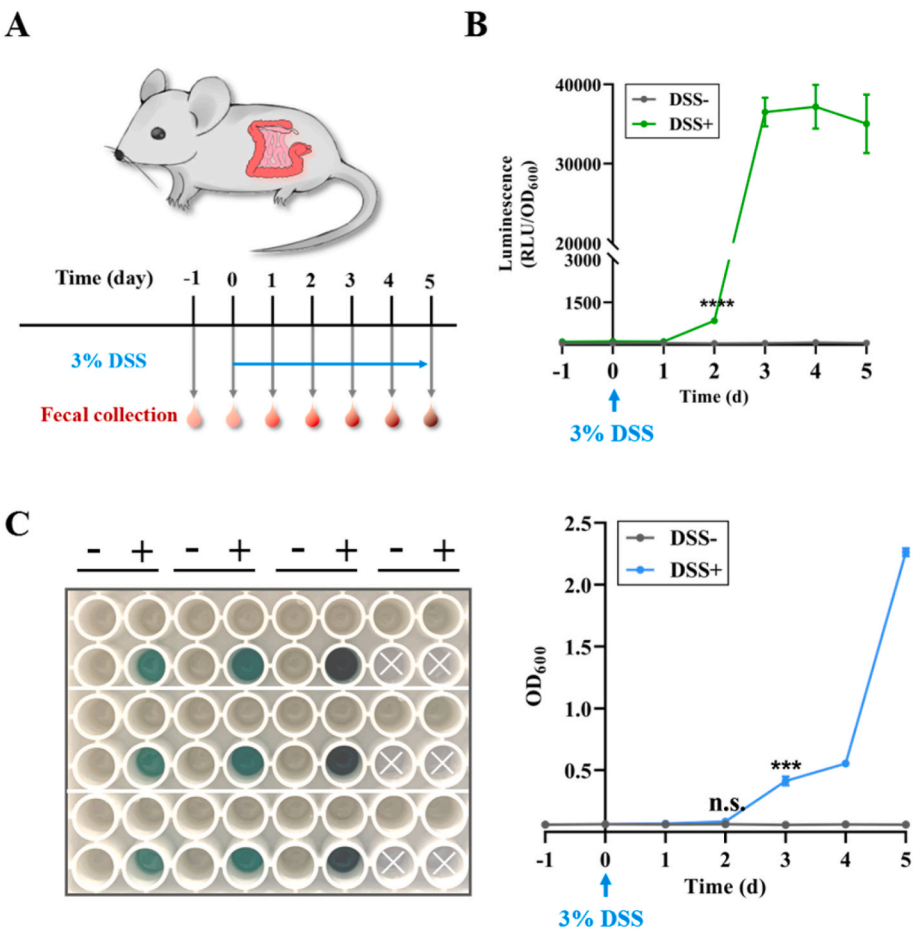


**Fig. 4.** Whole-cell biosensor for detecting bloody stool in DSS-induced colitis mice model. (A) Schematic of stool sample collection schedule. (B) Treated fecal samples from different experimental mice induce luminescence in engineered bacteria. The samples were added to the medium containing 1/1000 YES601 at a ratio of 1/200 and cultured for 4 h to detect bioluminescence. (C) Detection of bloody stool by o-tolidine method. Left: The color change reflected the degree of blood in the stool, -: DSS-. +: DSS+, each well showed the results of a fecal sample from one mouse. Right: Using a microplate reader to read the $OD_{600}$ after the chemical reaction. The data are presented as the mean ± SEM (n=3). (n.s.) $p>0.05$, *$p\leq0.05$, **$p\leq0.01$, ***$p\leq0.001$, ****$p\leq0.0001$.

filtered to obtain the samples to be tested. Macroscopic blood in the samples were observed only on the last day (Fig. S8). The samples were added to the medium containing 1/1000 YES601 at a ratio of 1/200 and cultured for 4 h to detect bioluminescence. Fig. 4B showed that the fecal samples on the second day after processing with DSS were able to significantly enhanced the luminescence signal, and there was no signal from healthy mice. In order to further prove the performance advantages of our WCB, we compared with two commercially commonly used chemical methods, o-tolidine method and pyramidon method (Fig. S9). The o-tolidine method exhibited a more obvious color reaction compared with pyramidon when the samples containing 7.5 ppm blood. Consequently, we used the o-tolidine method as the control. We added 50 μL of o-tolidine and 50 μL of $H_2O_2$ into 1 μL of the samples, respectively, and then recorded $OD_{600}$ after 5min incubation (Fig. 4C). This method could only detect bloody stool on the third day of DSS treatment. Based on these results, we considered that YES601 could detect fecal occult blood at an earlier stage of colitis compared to the o-tolidine method (Fig. 4B, C).

### 3.5. YES601 strain for ultrasensitive blood detection in human urine

Urine of a healthy person should be with none or very few RBCs (Coresh et al., 2003). People are considered to have hematuria if the number of RBCs is more than 3–5 per high-powered field (HPF) microscopy, which equates to $1 \times 10^4$ RBCs/mL of urine, and RBCs detection in the urine suggested the possibility of serious diseases in body, such as kidney disease, urinary tract infection or bladder cancer (Feld et al., 1997). Thus, accurate detection of hematuria is important for the diagnosis of urinary system diseases. To investigate the YES601's ability of detecting the trace amounts of blood in human urine, we added different concentrations of lysed blood to human urine containing 2.5% LB and then inoculated 1/1000 YES601 to the solution. The luminescent signals and $OD_{600}$ of the cultures were tested at 4 h (Fig. 5A, B). The luminescence signal results showed that the YES601 strain could detect blood as low as 0.25 ppm in human urine, which was equivalent to $1.25 \times 10^3$ RBCs per mL of human urine. The o-tolidine method was only able to detect blood ≥7.5 ppm in human urine samples (Fig. 5C). Lastly, we examined the time-response of YES601 in human urine under the induction of 0.625 and 1.25 ppm blood, and both concentrations were lower than the minimum detection limit of chemical methods. When exposed to blood, the significant bioluminescence signals could be observed in 40–50 min (Fig. 5D). Therefore, YES601 could detect hemorrhage in urine more sensitively than the chemical method, and the detection time was within an acceptable range for real applications, although human urine has some effect on the growth of YES601 (Fig. S10).

Whole-cell biosensor should be stable for a considerable period of time to meet practical applications. We reactivated YES601 strain which has been stored at −80 °C for more than 6 months and tested its detection performance. The results showed that YES601 was still able to detect lysed blood (2 ppm) contained in medium within 1 h sensitively (Fig. S11A). We also freeze-dried YES601 strain and stored it at 4 °C for one or two weeks (Fig. S11B), then the strain was reactivated on the seventh and fourteenth day to test its ability responding to the lysed blood respectively. This result also indicated that freeze-dried YES601 was able to detect trace amounts of blood (2 ppm) after reactivation (Figs. S11C and D).

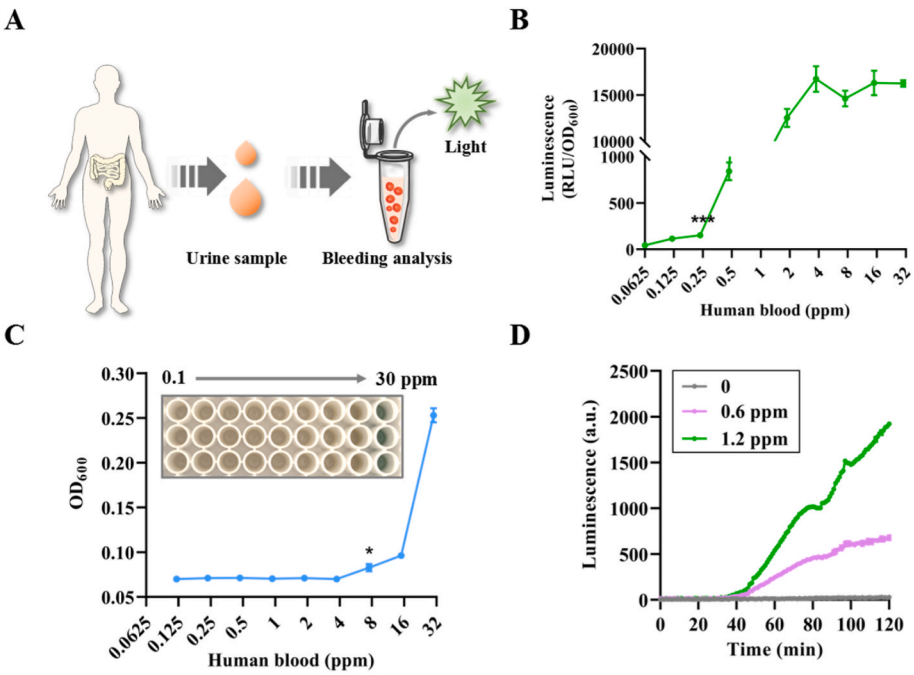


**Fig. 5.** Detecting blood in human urine by YES601. (A) Schematic diagram of the detection process. (B) Different concentrations of blood in urine induce luminescence of engineered bacteria. The bacteria cells were exposed to human urine containing 2.5% LB dissolved and various lysed blood. (C) Detection of hematuria by o-tolidine method. Urine samples containing 2.5% LB and various concentrations of blood. (D) Time-responses of YES601 after exposure to various lysed blood concentrations in human urine, and bioluminescence signals were read at 1 min intervals for 120 min. The data are presented as the mean ± SEM (n=3). (n.s.) $p>0.05$, *$p\leq0.05$, **$p\leq0.01$, ***$p\leq0.001$, ****$p\leq0.0001$.

## 4. Conclusions

Well-designed and customized WCBs possess great potential to be alternatives of the traditional detection methods. In this study, we designed a WCB, named YES601, for ultrasensitive detection of heme/lysed blood by systematically reprogrammed a heme-responsive gene circuit. Our biosensor exhibited a satisfied MIR (more than 4000 folds) and improved detection limit (0.12 ppm) in LB medium, which is 62.5-fold lower than o-tolidine method (7.5 ppm). More importantly, YES601 could detect fecal occult blood metabolized by DSS-induced mice on the second day, while o-tolidine method was only present in the third day sample. In human urine samples, the minimum detection limit of lysed blood by YES601 was 0.25 ppm, which was much more sensitive compared with the o-tolidine method (≥7.5 ppm). In addition, YES601 could detect as low as 1 ppm of lysed blood in human urine at 60 min which was within an acceptable range for practical applications. Taken together, YES601 is expected to be developed into a commercial kit for ultrasensitive detection of heme and further developed into a tool for microbleeding site diagnosis *in vivo*.

## CRediT authorship contribution statement

**Zhen-Ping Zou:** Methodology, Data curation, Manuscript preparation. **Ying Yang:** Methodology, Data curation. **Junshan Wang:** Methodology. **Ying Zhou:** Conceptualization, Project administration, Writing – review & editing. **Bang-Ce Ye:** Conceptualization, Project administration, Funding acquisition, Writing – review & editing.

## Declaration of competing interest

The authors declare that they have no known competing financial interests or personal relationships that could have appeared to influence the work reported in this paper.

## Data availability

Data will be made available on request.

## Acknowledgments

This wok was sponsored by the National Key Research and Development Program of China (2020YFA0908800) and the National Natural Science Foundation of China (22134003).

## Appendix A. Supplementary data

Supplementary data to this article can be found online at https://doi.org/10.1016/j.bios.2022.114520.

## References

Barger, N., Litovco, P., Li, X., Habib, M., Daniel, R., 2019. Nucleic Acids Res. 47 (19), 10464–10474.
Barger, N., Oren, I., Li, X., Habib, M., Daniel, R., 2021. ACS Synth. Biol. 10 (5), 1132–1142.
Cameron, D.E., Collins, J.J., 2014. Nat. Biotechnol. 32, 1276.
Cayron, J., Prudent, E., Escoffier, C., Gueguen, E., Mandrand-Berthelot, M.A., Pignol, D., Garcia, D., Rodrigue, A., 2017. Environ. Sci. Pollut. Res. Int. 24 (1), 4–14.
Chen, Y., Ho, J.M.L., Shis, D.L., Gupta, C., Long, J., Wagner, D.S., Ott, W., Josić, K., Bennett, M.R., 2018. Nat. Commun. 9, 64.
Clifton, K.P., Jones, E.M., Paudel, S., Marken, J.P., Monette, C.E., Halleran, A.D., Epp, L., Saha, M.S., 2018. J. Biol. Eng. 12, 23.
Close, D., Xu, T., Smartt, A., Rogers, A., Crossley, R., Price, S., Ripp, S., Sayler, G., 2012. Sensors 12 (1), 732–752.
Coresh, J., Astor, B.C., Greene, T., Eknoyan, G., Levey, A.S., 2003. Am. J. Kidney Dis. 41 (1), 1–12.
Ding, N., Zhou, S., Deng, Y., 2021. ACS Synth. Biol. 10 (5), 911–922.
Feld, L.G., Waz, W.R., Pérez, L.M., Joseph, D.B., 1997. Pediatr. Clin. North. Am. 44 (5), 1191–1210.
Flynn, S., Eisenstein, S., 2019. Surg. Clin. 99 (6), 1051–1062.
Freni, S.C., Heederik, G.J., Hol, C., 1977. J. Clin. Pathol. 30 (4), 336–340.
Gardner, T.S., Cantor, C.R., Collins, J.J., 2000. Nature 403 (6767), 339–342.
Hicks, M., Bachmann, T.T., Wang, B., 2020. ChemPhysChem 21 (2), 131.
Hossain, G.S., Saini, M., Miyake, R., Ling, H., Chang, M.W., 2020. Trends Biotechnol. 38 (7), 797–810.
Hynninen, A., Tönismann, K., Virta, M., 2020. Bioeng. Bugs 1 (2), 132–138.
Javanpour, A.A., Liu, C.C., 2021. ACS Synth. Biol. 10 (10), 2705–2714.
Jiang, W., He, X., Luo, Y., Mu, Y., Gu, F., Liang, Q., Qi, Q., 2020. ACS Synth. Biol. 9 (9), 2588–2599.
Knippel, R.J., Zackular, J.P., Moore, J.L., Celis, A.I., Weiss, A., Washington, M.K., DuBois, J.L., Caprioli, R.M., Skaar, E.P., 2018. PLoS Pathog. 14 (12), e1007486.
Landry, B.P., Tabor, J.J., 2017. Microbiol. Spectr. 5 (5).
Lechardeur, D., Cesselin, B., Liebl, U., Vos, M.H., Fernandez, A., Brun, C., Gruss, A., Gaudu, P., 2012. J. Biol. Chem. 287 (7), 4752–4758.
Lopreside, A., Wan, X., Michelini, E., Roda, A., Wang, B., 2019. Anal. Chem. 91 (23), 15284–15292.

Mandel, J.S., Church, T.R., Bond, J.H., Ederer, F., Geisser, M.S., Mongin, S.J., Snover, D. C., Schuman, L.M.N., 2000. Engl. J. Med. 343 (22), 1603–1607.
Meighen, E.A., 1991. Microbiol. Rev. 55 (1), 123–142.
Mimee, M., Nadeau, P., Hayward, A., Carim, S., Flanagan, S., Jerger, L., Collins, J., McDonnell, S., Swartwout, R., Citorik, R.J., Bulović, V., Langer, R., Traverso, G., Chandrakasan, A.P., Lu, T.K., 2018. Science 360 (6391), 915–918.
Mitchler, M.M., Garcia, J.M., Montero, N.E., Williams, G.J., 2021. Curr. Opin. Biotechnol. 69, 172–181.
Moraskie, M., Roshid, M.H.O., O'Connor, G., Dikici, E., Zingg, J.M., Deo, S., Daunert, S., 2021. Biosens. Bioelectron. 191, 113359.
Nasir, N., Raji, S., Mustafa, F., Rizvi, T.A., Natour, Z.A., Hilal-Alnaqbi, A., Ahmad, M.A., 2019. Heliyon 6 (1), e03102.
Nielsen, A.A.K., Der, B.S., Shin, J., Vaidyanathan, P., Paralanov, V., Strychalski, E.A., Ross, D., Densmore, D., Voigt, C.A., 2016. Science 352 (6281) aac734.
Nishinaga, M., Sugimoto, H., Nishitani, Y., Nagai, S., Nagatoishi, S., Muraki, N., Tosha, T., Tsumoto, K., Aono, S., Shiro, Y., Sawai, H., 2021. Commun. Biol. 4 (1), 467.
Nobles, C.L., Clark, J.R., Green, S.I., Maresso, A.W., 2015. J. Microbiol. Methods 118, 7–17.
Riglar, D.T., Silver, P.A., 2018. Nat. Rev. Microbiol. 16 (4), 214–225.
Roquet, N., Lu, T.K., 2014. Biotechnol. J. 9 (5), 597–608.
Sahu, S., Roy, R., Anand, R., 2022. ACS Sens. 7 (3), 704–715.
Saillant, V., Lipuma, D., Ostyn, E., Joubert, L., Boussac, A., Guerin, H., Brandelet, G., Arnoux, P., Lechardeur, D., 2021. mBio 12 (1), e03392-20.
Schladt, T., Engelmann, N., Kubaczka, E., Hochberger, C., Koeppl, H., 2021. ACS Synth. Biol. 10 (12), 3316–3329.
Tang, W., Liu, D.R., 2018. Science 360 (6385), eaap8992.
Tas, H., Grozinger, L., Stoof, R., Lorenzo, V., Goñi-Moreno, Á., 2021. Nat. Commun. 12 (1), 355.
Valle, I.D., Fulk, E.M., Kalvapalle, P., Silberg, J.J., Masiello, C.A., Stadler, L.B., 2020. Front. Microbiol. 11, 618373.
Veerreddy, P., 2013. Clin. Med. Insights Blood Disord. 6, 7–17.
Wan, X., Ho, T.Y.H., Wang, B., 2019a. Handb. Cell Biosens, p. 1.
Wan, X., Pinto, F., Yu, L., Wang, B., 2020. Nat. Commun. 11 (1), 5961.
Wan, X., Volpetti, F., Petrova, E., French, C., Maerkl, S.J., Wang, B., 2019b. Nat. Chem. Biol. 15 (5), 540–548.
Westendorf, A.M., Gunzer, F., Deppenmeier, S., Tapadar, D., Hunger, J.K., Schmidt, M. A., Buer, J., Bruder, D., 2005. FEMS Immunol. Med. Microbiol. 43, 373–384.
Yagur-Kroll, S., Belkin, S., 2011. Anal. Bioanal. Chem. 400 (4), 1071–1082.
Zhou, Z., Chen, X., Sheng, H., Shen, X., Sun, X., Yan, Y., Wang, J., Yuan, Q., 2020. Microb. Cell Factories 19 (1), 56.
Zou, Z.P., Ye, B.C., 2020. ACS Synth. Biol. 9 (9), 2440–2449.